ISSN: 0128-7680
Pertanika J. Sci. & Technol. **16 (1)**: 41 - 48 (2008)

Growth of Gold Particles on Glassy Carbon from a Thiosulphate-Sulphite Aged Electrolyte

S. Sobri*[1], S. Roy[2], E. Kalman[3], P. Nagyp[3] and M. Lakatos[4]

[1]*Department of Chemical and Environmental Engineering, Faculty of Engineering, Universiti Putra Malaysia, 43400 UPM, Serdang, Selangor, Malaysia*

[2]*School of Chemical Engineering and Advanced Materials, Merz Court, University of Newcastle upon Tyne, NE1 7RU, UK*

[3]*Chemical Research Centre of the Hungarian Academy of Sciences (CHEMRES), H-1025 Budapest, Pusztaszeri ut 59-67, Hungary*

[4]*Institute for Materials Science and Technology of the Bay Zolt·n Foundation (BAYATI), H-1116 Budapest, Fehervari ut. 130, Hungary*

**E-mail: eeza@eng.upm.edu.my*

ABSTRACT

Interest has grown in developing non-toxic electrolytes for gold electrodeposition to replace the conventional cyanide-based bath for long term sustainability of gold electroplating. A solution containing thiosulphate and sulphite has been developed specially for microelectronics applications. However, at the end of the electrodeposition process, the spent electrolyte can contain a significant amount of gold in solution. This study has been initiated to investigate the feasibility of gold recovery from a spent thiosulphate-sulphite electrolyte. This paper presents the microscopy observations of crystal growth of gold on glassy carbon as a function of deposition potentials and time. It was found that the initial deposition of gold at less cathodic potential corresponds to an electrochemical diffusion control of gold discharge from which spherical nuclei are obtained. When a certain induction time for spherical growth has passed, the initial growing nuclei become unstable and the thin gold deposit begins to develop tips which eventually grow larger and produce dendrites. The dendritic growth is controlled by surface diffusion limitations of gold nuclei.

Keywords: Gold electrodeposition, thiosulphate-sulphite, glassy carbon

INTRODUCTION

The emerging use of gold-based connectors in microtechnology has initiated the need to search for stable and non-toxic electrolytes for gold electrodeposition because the classical cyanide-based bath has been found to be incompatible with positive photoresists used during the process (Osaka *et al.,* 2001; Liew *et al.*, 2003, Green *et al.*, 2003; Liew, 2002; Watanabe *et al.*, 1999). One electrolyte being examined is a solution containing thiosulphate and sulphite, which was initially proposed by Osaka *et al.* (2001). This electrolyte was reported to be highly stable, requires no stabilizing additives and contained phosphoric acid as buffering agent.

Recently, a mixed thiosulphate-sulphite ligand bath has been formulated by Newcastle University with aurochloric acid, Au (III) Cl^{-4}, as the starting material (Liew *et al.*, 2003). Subsequent reduction and complexation by thiosulphate led to the formation of

* Corresponding Author

$Au(S_2O_3)_2^{3-}$. This electrolyte was found to be stable at near neutral pH and showed good compatibility with positive photoresists (Green *et al.*, 2003). The mixed ligand bath proved to be satisfactory for an industrial process and is used as electrolyte to electrodeposit gold for microelectronics applications.

Since the discharge of gold with effluent is a major economic and environmental concern, this study was carried out to investigate whether gold can be recovered from aged thiosulphate-sulphite electrolyte and to determine the microstructure of the deposits/particles obtained. Currently, there is no reliable information concerning gold recovery from thiosulphate-sulphite plating baths. The recovery process is expected to be of value if the recovered gold can be tailored for suitable applications, for example in catalysis, sensors, electronics and others (Hutchings, 1996; Corti *et al.*, 2002; Goodman, 2002).

In a previous work to investigate the nucleation mechanism of gold (Sobri and Roy, 2005), glassy carbon and graphite had been used as electrodes. The two forms of carbon were chosen due to the differences in their structures. It was found that at the early stages of the reduction process, the deposition of gold on glassy carbon exhibits an instantaneous nucleation of non-overlapping particles. At longer times, the particles begin to overlap and the deposition follows a classic progressive nucleation phenomenon. Deposition of gold on graphite, however, does not follow the classical nucleation phenomenon.

MATERIALS AND METHODS

Glassy carbon (Goodfellow Cambridge Ltd, UK) was used as the electrode. The substrate was 99.5% pure with 1 mm thickness. The electrode was cut into 1 cm^2 and attached to a copper wire using silver loaded epoxy adhesive and hardener (RS Components, UK). In order to avoid metal deposition on copper wire and silver paste used for contact, the metallic area was covered with multi-purpose silicone sealant (Dow Corning Ltd, UK).

Gold was deposited from the thiosulphate-sulphite aged electrolyte. Details on electrolyte preparation are reported in Liew *et al.* (2003). The bath mainly consist of $Au(S_2O_3)_2^{3-}$ as well as trace amounts of Na^+ ions. The concentration of the predominant species, Au+, was 8.981 g/L. The electrochemical experiments were performed in a three-electrode H-cell. The cell was separated into anode and cathode compartments by a glass frit. 45 ± 1 ml volume of aged gold thiosulphate-sulphite plating solution was equally divided in each compartment.

A potentiostat (Sycopel Scientific) controlled by a computer was used to carry out the experiments. The working electrode was mounted in the cell and held in place by the use of a metal clip. 2.0 × 2.5 cm^2 platinised-titanium sheet was used as the auxiliary electrode. All potential measurements were made with respect to a saturated mercurous sulphate electrode (SMSE).

Current-time transients were accomplished by applying the potentials from the rest potential to the deposition potentials of lower than –0.7 V for 60 seconds. Prior to each chronoamperometry measurements, the carbon surface was gently polished using wet silicon carbide paper grit 4000 (Struers Ltd., UK) and then washed thoroughly with distilled water before being transferred to the experimental cell.

In order to study the growth of gold with time, a set of current-time transients were accomplished by applying the potentials from the rest potential to the deposition potentials of –0.925 V and –1.20 V, for durations of 1, 10, 100, 500 and 1000 seconds. The two deposition potentials were chosen as it shows transition from growth of single particulates to aggregates. Atomic Force Microscopy (AFM) analysis for gold deposits was

recorded using a Nanoscope Dimension™ 3100 with operational frequency of 2 Hz. The AFM was operated in contact mode, scanning at 25 mm imaging resolutions. Scanning Electron Microscopy (SEM) analysis was also performed using a Hitachi model SE570 SEM at an acceleration voltage of 20 kV.

RESULTS AND DISCUSSION

Fig.1 contains representative scanning electron micrographs of gold nanoparticles on glassy carbon after 60 seconds of potential application. These images illustrate the influence of overpotentials on crystal distribution and size. As shown in the images, deposition at –0.775 V yields a smaller number of nuclei. Notably, the nuclei are of nearly the same size, the average size being 680 ±10 nm. At intermediate overpotential, two distinct nuclei sizes are visible, with average particle sizes of 650 nm and 160 nm. As the applied potential is lowered, homogeneous nanocrystals ranging in diameter from 80 to 100 nm are obtained. A manual image analysis showed that the range of crystal diameter had a relative deviation of less than 1% for potentials below –1.0 V.

Fig. 2 contains representative atomic force micrographs of gold nanoparticles on glassy carbon at 25 mm resolution. These images illustrate the distribution of gold nuclei at an overpotential of –0.925 V after 1s, 10s, 100s, 500s and 1000s deposition

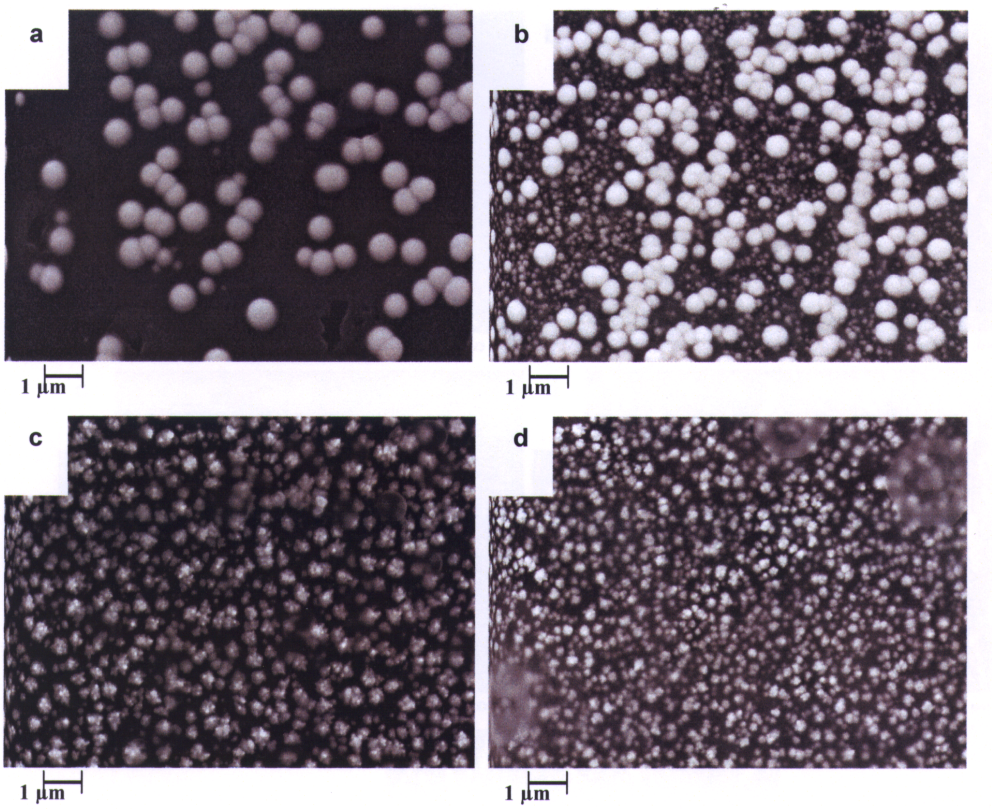

Fig. 1: SEM images of gold on glassy carbon as a function of deposition overpotentials: (a) –0.775 (b) –0.925 (c) –1.075 (d) –1.20V

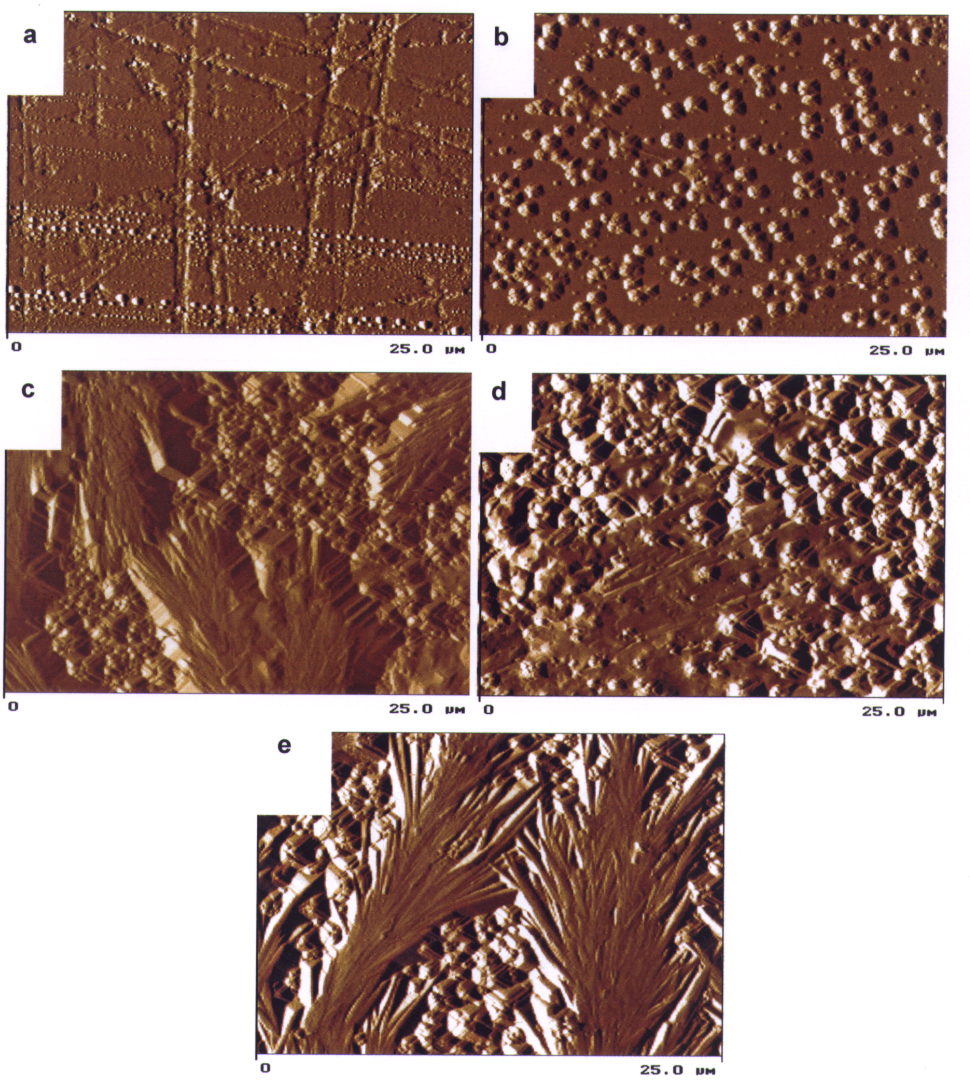

Fig. 2: AFM images of gold on glassy carbon at –0.925V at (a) 1s (b) 10s (c) 100s (d) 500s (e) 1000s

time. As shown in the images, deposition at 1s yields a number of large nuclei. During this stage, each nuclei grows independently of each other. These gold nuclei deviate little in size, with average size of 120 nm. Between 1s and 10s, a fraction of the gold nuclei begin to coalesce while some remain as single particle. The average size of gold aggregates is 550 nm.

Deposition at longer periods results in complete coverage of gold aggregates on the substrate surface. The particles are clustered into larger aggregates and measurement of the diameter of the particles or aggregates was not possible. The 3-D images in *Fig. 3* demonstrate the changes in surface feature from single particulates at 1s to smooth gold deposits at 1000s.

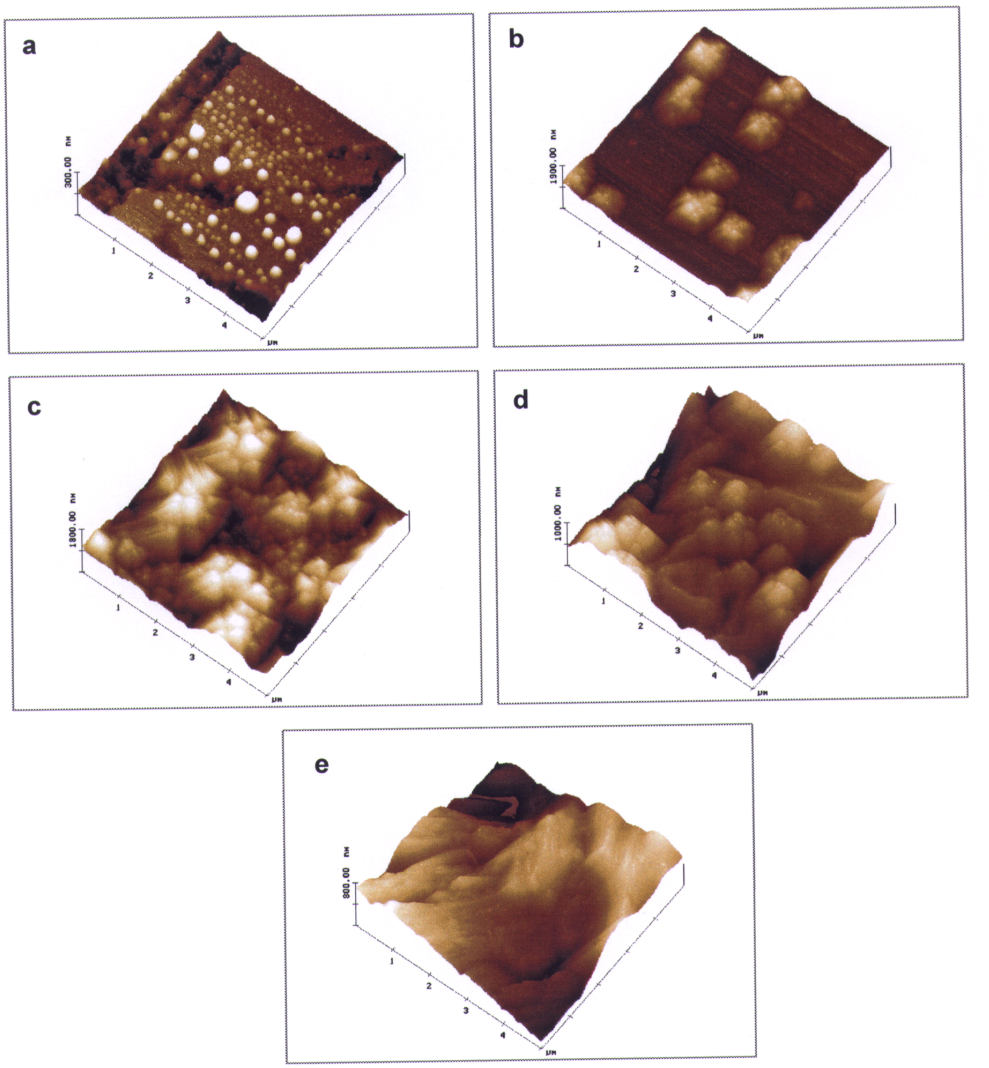

Fig. 3: 3–dimensional images of gold on glossy carbon at –0.925V at (a) 1s (b) 10s (c) 100s (d) 500s (e) 1000s

Fig. 4 represents the micrographs of gold nanoparticles on glassy carbon deposited at an overpotential of –1.20 V and 25 mm imaging resolution. The images presented indicate that the growth of gold nuclei exhibits a needle-like structure which occurs even before the first second had elapsed.

In order to determine the density of gold nuclei as a function of overpotential, 15 μm^2 areas were randomly chosen from the micrographs of the substrate surface with each of the area being $1\mu m^2$. The values are listed in Table 1. The density of nuclei increased with increasing overpotential for gold reduction. These nuclei density values are an order of magnitude 10^1–10^2 smaller compared to those reported for gold deposition from chlorides (Schmidt *et al.*, 1997), which could be due to the difficulty of reduction from sulphite based electrolytes.

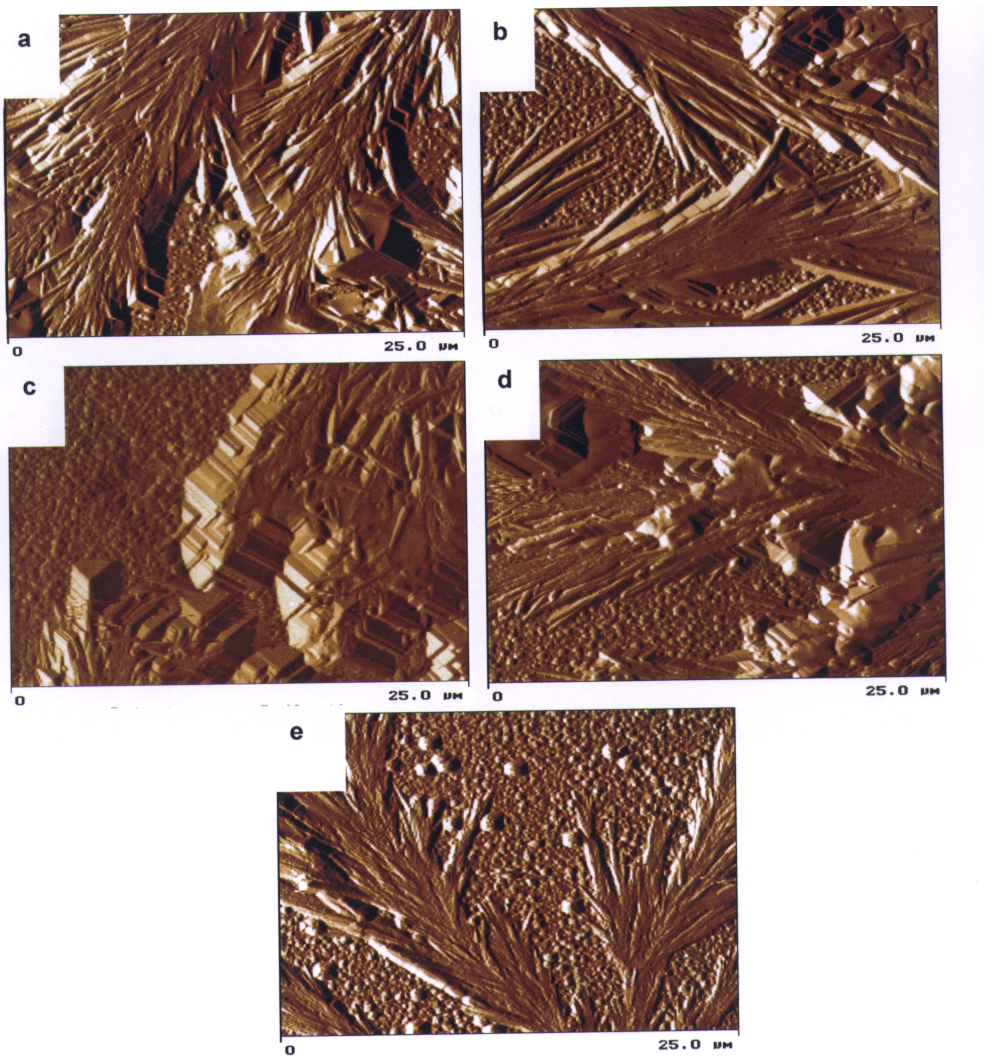

Fig. 4: AFM images of gold on glassy carbon at –1.20V at (a) 1s (b) 10s (c) 100s (d) 500s (e) 1000s

TABLE 1
Nuclei density of gold glassy carbon as a function overpotential

η(V)	Average particle density calculated from SEM (10^{-8}/cm^{-2})
–0.775	4
–0.925	8
–1.075	13
–1.200	19

The microscopy images at more negative overpotentials indicate that the growth of gold nuclei exhibits a needle-like structure. This characteristic was affirmed by the observed microscopy images at 200 magnifications, as shown in *Fig. 5*. Each 'branch' is formed from a nucleus or centre of crystallisation, which proceeds to send out radial arms. From these primary arms, secondary and tertiary arms begin to sprout and this is repeated until a surface pattern, known as dendrites, is formed on the surface. These gold dendrites develop by the addition of nuclei onto its branches.

It can also be seen that the dendrites arms grow outward and thickened as the deposition time increased. They continue to grow until its outer arms are in contact with neighbouring dendrites, in which this contact acts as a boundary of the grain. Further growth results in thickening of the existing dendrites arms, as can be seen from *Fig. 5*. Images recorded both by AFM and SEM, revealed that the spaces between the dendrites arms are also ultimately filled with particles.

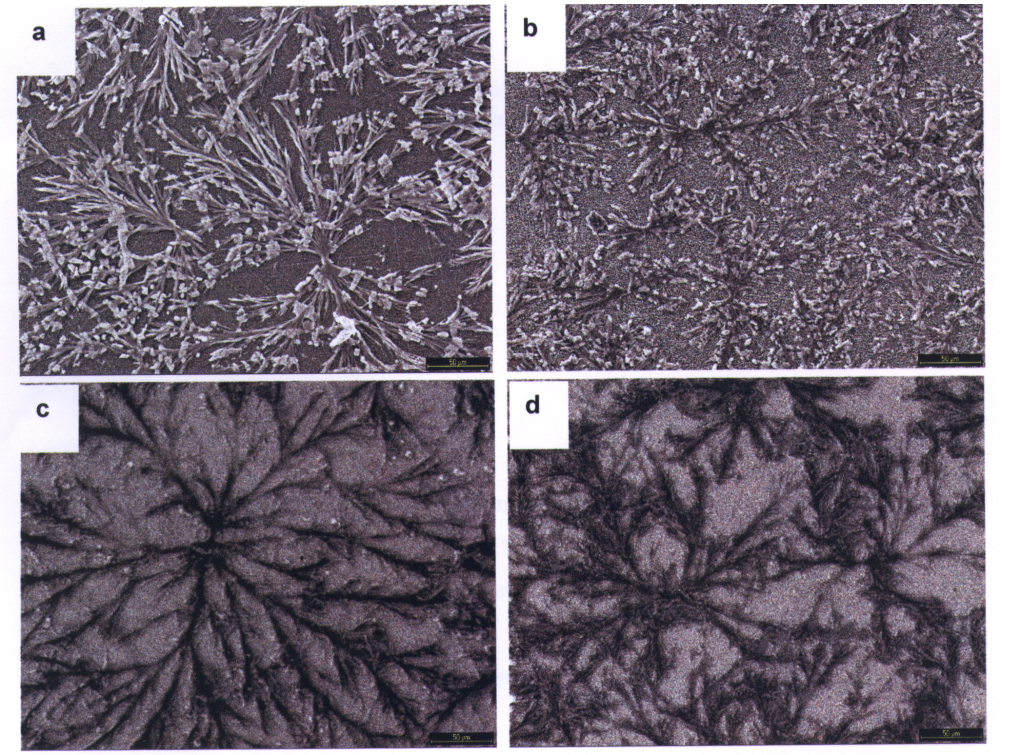

Fig. 5: SEM images of gold on glassy carbon at –1.20V at (a) 10s (b) 100s (c) 500s (d) 1000s

CONCLUSIONS

The electrodeposition of gold was studied from gold thiosulphate-sulphite aged electrolyte. Electrochemistry and microscopy analysis were applied to characterize Au^{+} crystals deposited on the carbon substrates. Microscopy observations demonstrated that the particle size and density can be controlled by varying the deposition potentials and time.

Deposition at less cathodic overpotentials yields a smaller number of large particles. As the applied potential is lowered, homogenenous Au crystals ranging in diameter from 80-100 nm are obtained. The particle density increases with overpotential, signifying the increase in number of nucleation sites. It is also evident that single crystals can be obtained shortly after applying a potential whereas at longer times the particle tend to coalesce and form larger aggregates with diameters ranging from 100 to 300 nm. AFM images also show that the growth of gold nuclei at more cathodic overpotential exhibits a needle-like structure and the substrate is ultimately filled with gold aggregates.

ACKNOWLEDGEMENTS

S. Sobri acknowledges a Short Term Scientific Mission (STSM) grant from COST D19-00935. The work was carried out in a facility funded by JIF-4NESCEQ grant. Grant Staines, D. Arranyi and K. Papp helped with SEM and AFM measurements.

REFERENCES

Corti, C.W., Holliday, R.J. and Thompson, D.T. (2002). Developing new industrial applications for gold: Gold nanotechnology. *Gold Bull. (Geneva), 35*(4), 111.

Goodman, P. (2002). Current and future uses of gold in electronics. *Gold Bull. (Geneva), 35*(1), 21.

Green, T.A., Liew, M.J. and Roy, S. (2003). Electrodeposition of gold from a thiosulfate-sulfite bath for microelectronic applications. *J. Electrochem. Soc., 150,* C104.

Hutchings, G.J. (1996). Catalysis: A golden future. *Gold Bull. (Geneva), 29*(4), 123.

Liew, M.J. (2002, July). Title of thesis. (PhD Thesis, University of Newcastle upon Tyne, UK, 2002).

Liew, M.J., Roy, S. and Scott, K. (2003). Development of a non-toxic electrolyte for soft gold electrodeposition: An overview of work at University of Newcastle upon Tyne. *Green Chem., 5,* 376.

Osaka, T., Kato, M., Sato, J., Yoshizawa, K., Homma, T., Okinaka, Y. and Yushioka, O. (2001). Mechanism of sulfur inclusion in soft gold electrodeposited from the thiosulfate-sulfite bath. *J. Electrochem. Soc., 148,* C659.

Schmidt, U., Donten, M. and Osteryoung, J.G. (1997). Gold electrocrystallization on carbon and highly oriented pyrolytic graphite from concentrated solutions of LiCl. *J. Electrochem. Soc., 144,* 2013.

Sobri, S. and Roy, S. (2005). Gold electrocrystallization from a spent thiosulfate-sulfite electrolyte. *J. Electrochem. Soc., 152,* C593.

Watanabe, H., Hayashi, S. and Honma, H. (1999). Microbump formation by noncyanide gold electroplating. *J. Electrochem. Soc., 146,* 574.